Nuclear excitation by electronic transition of ^{235}U

P. A. Chodash,[1,*] J. T. Harke,[2] E. B. Norman,[1] S. C. Wilks,[3] R. J. Casperson,[2] S. E. Fisher,[4] K. S. Holliday,[5] J. R. Jeffries,[5] and M. A. Wakeling[6]

[1]*Department of Nuclear Engineering, University of California, Berkeley, California 94720, USA*
[2]*Nuclear and Chemical Sciences Division, Lawrence Livermore National Laboratory, Livermore, California 94550, USA*
[3]*Physics Division, Lawrence Livermore National Laboratory, Livermore, California 94550, USA*
[4]*National Security Engineering Division, Lawrence Livermore National Laboratory, Livermore, California 94550, USA*
[5]*Materials Science Division, Lawrence Livermore National Laboratory, Livermore, California 94550, USA*
[6]*Air Force Institute of Technology, Wright-Patterson Air Force Base, Ohio 45433, USA*

(Received 15 December 2015; published 11 March 2016)

Background: Nuclear excitation by electronic transition (NEET) is a rare nuclear excitation that can occur in isotopes containing a low-lying nuclear excited state. Over the past 40 yr, several experiments have attempted to measure NEET of ^{235}U and those experiments have yielded conflicting results.
Purpose: An experiment was performed to determine whether NEET of ^{235}U occurs and to determine its excitation rate.
Method: A pulsed Nd:YAG laser operating at 1064 nm with a pulse energy of 790 mJ and a pulse width of 9 ns was used to generate a uranium plasma. The plasma was collected on a catcher plate and electrons from the catcher plate were accelerated and focused onto a microchannel plate detector. An observation of a decay with a 26-min half-life would suggest the creation of ^{235m}U and the possibility that NEET of ^{235}U occurred.
Results: A 26-min decay consistent with the decay of ^{235m}U was not observed and there was no evidence that NEET occurred. An upper limit for the NEET rate of ^{235}U was determined to be $\lambda_{\mathrm{NEET}} < 1.8 \times 10^{-4}$ s^{-1}, with a confidence level of 68.3%.
Conclusions: The upper limit determined from this experiment is consistent with most of the past measurements. Discrepancies between this experiment and past measurements can be explained by assuming that past experiments misinterpreted the data.

DOI: 10.1103/PhysRevC.93.034610

I. INTRODUCTION

Nuclear excitation by electronic transition (NEET) was first predicted by Morita in 1973 [1]. This process refers to a coupling between an electronic transition and a nuclear transition, which allows for the nucleus to be excited and is the inverse of bound internal conversion. Possible candidate isotopes for NEET are limited owing to the requirement of low-lying nuclear excited states. This requirement is a consequence of electronic transitions typically having lower energy than nuclear transitions. Because it was predicted, numerous experiments to measure NEET in a variety of isotopes were conducted [2–13]. Many of those experiments yielded conflicting results and the results differed significantly from theoretical estimates. Measurements on ^{197}Au and ^{193}Ir have provided evidence of NEET occurring and the results were near theoretical estimations [2–4]. One candidate isotope, ^{235}U, has a low-lying isomeric state at 76 eV and has been studied several times over the past 40 yr. The isomeric state, denoted hereafter by ^{235m}U, decays by internal conversion with a half-life of approximately 26 min. The half-life is not precisely known owing to the chemical environment affecting the internal conversion decay [14–16]. Several experiments have been performed looking for NEET of ^{235}U and they have produced conflicting results [5–8].

The very first experiment was performed by Izawa *et al.* in 1979 [5,6]. A transversely excited atmospheric CO_2 laser with a pulse energy of 1 J and a pulse width of 100 ns irradiated a sample of natural uranium (NU) metal. The ablated material was caught on a plate, and a channel electron multiplier detector was used to measure low-energy electrons. Two decay curves were observed along with a constant background. The fast decay with a half-life of 1.0 ± 0.1 min was attributed to α emission from material not collected on the collection plate, and the slow decay with a half-life of 25.7 ± 0.4 min was attributed to the decay of ^{235m}U. The Maxwellian averaged cross section for NEET was determined to be $\langle \sigma_N v \rangle = 1.4 \times 10^{-20}$ cm^3/s, which can be converted to an excitation rate of approximately 0.1 s^{-1} [18].

The next set of experiments was performed by Arutyunyan *et al.* [7]. The first experiment was similar to Izawa *et al.* A 5-J CO_2 laser with a 200-ns pulse width was used to irradiate a 6% enriched UO_2 ceramic target, and a channel electron multiplier was used to detect low-energy electrons. No signal for the decay of ^{235m}U was observed, even though the target was enriched in ^{235}U. The NEET cross section was determined to be $\sigma_{\mathrm{NEET}} < 10^{-32}$ cm^2. The second experiment performed used a high-energy electron gun to create the uranium plasma. An electron beam composed of 500-keV electrons with a beam current of 150 kA and a pulse duration of 30 ns was used. A variety of uranium targets with enrichment spanning depleted uranium (DU) up to 99.99% highly enriched uranium (HEU) were used. Only the two targets with enrichment

*Present address: Lawrence Livermore National Laboratory, Livermore, California 94550, USA.

greater than 90% produced a signal consistent with the decay of ^{235m}U. The NEET cross section was calculated to be $\sigma_e = 1 \times 10^{-32}$–$1 \times 10^{-31}$ cm^2, which is equivalent to an excitation rate of 3×10^{-5} s^{-1} [18].

The most recent experiment looking for NEET of ^{235}U was performed by Claverie *et al.* [8]. A 1-J Nd:YAG laser with a pulse width of 5 ns was used to irradiate a sample of 93% enriched uranium with an estimated power density on target of approximately 10^{13} W/cm^2. The uranium plume was captured on a gold catcher plate and a channeltron detector was used to measured the low-energy electrons emitted from the plate. The experiment did not observe a decay signal and an upper limit for NEET of ^{235}U was determined to be $\lambda_{\mathrm{NEET}} < 6 \times 10^{-6}$ s^{-1}.

This paper reports the latest experiment to determine if NEET of ^{235}U occurs and at what rate. Similar to past experiments, a high-intensity laser was used to generate a plasma that was subsequently captured on a catcher plate. An electron detector was used to determine if ^{235m}U was produced. Section II describes the theory for NEET of ^{235}U along with plasma simulations performed to predict the amount of ^{235m}U generated within the uranium plasma. The experimental setup is described in detail in Sec. III. The results from the various experimental runs are described in Sec. IV. Section V discusses the results from this experiment and compares them to the results of previous measurements looking for NEET of ^{235}U. Section VI provides concluding remarks and discusses improvements necessary for future measurements. Further details for the experiment can be found in Ref. [17].

II. NEET THEORY AND SIMULATIONS

Ever since NEET was first proposed in 1973, numerous papers have attempted to calculate NEET rates for a variety of candidate isotopes [1,18–25]. NEET theory involves a combination of atomic theory, nuclear theory, and plasma theory. In the case of uranium, numerous electronic configurations and transitions within an evolving plasma make accurate modeling difficult. For NEET to occur, the energy of the atomic transition has to overlap the energy of the nuclear transition. In addition, differences in the multipolarity of the transitions significantly reduces the probability of NEET occurring. The NEET excitation rate is defined as

$$\lambda_{\mathrm{NEET}} = \sum_q \sum_{if} P^{q,i}(n_e,T)\lambda_A^{q,i}(n_e,T)P_{\mathrm{NEET}}^{q,i}(n_e,T), \quad (1)$$

where i is the initial atomic state, f is the final atomic state, q is the charge state within the plasma, T is the electron temperature in the plasma, n_e is the electron density in the plasma, $P^{q,i}(n_e,T)$ is the fraction of ions in a specific atomic configuration, $\lambda_A^{q,i}(n_e,T)$ is the atomic transition deexcitation rate, and $P_{\mathrm{NEET}}^{q,i}(n_e,T)$ is the probability for the NEET transition to occur. The importance of the energy mismatch and the atomic transition widths is clearly seen when the probability for the NEET transition is written as

$$P_{\mathrm{NEET}}^{q,i}(n_e,T) = \left(1 + \frac{\Gamma_f}{\Gamma_i}\right)\frac{V_{if}^2}{\delta_{if}^2 + \frac{1}{4}(\Gamma_f + \Gamma_i)^2}, \quad (2)$$

where Γ_i and Γ_f are the initial and final atomic state widths, δ_{if} is the energy mismatch between the nuclear and atomic transitions, and V_{if} is the matrix element for the nuclear-atomic coupling [18]. The matrix element accounts for the multipolarity difference between the nuclear and the atomic transition.

There are two papers that explicitly focused on NEET of ^{235}U. In Harston and Chemin [18], a laser-produced uranium plasma is modeled using a collisional-radiative model. Two electronic transitions that are expected to match the energy of the 76-eV nuclear transition are the $6p_{1/2} \rightarrow 5d_{5/2}$ transition and the $6d_{5/2} \rightarrow 6p_{1/2}$ transition. The model predicts that the $6p_{1/2} \rightarrow 5d_{5/2}$ transition occurs when the uranium is in a charge state 10+ and the $6d_{5/2} \rightarrow 6p_{1/2}$ transition occurs when the uranium is in a charge state of 23+. The $6d_{5/2} \rightarrow 6p_{1/2}$ transition is expected to have a larger NEET rate. Although the NEET rate is expected be larger for the $6d_{5/2} \rightarrow 6p_{1/2}$ transition, the higher charge state adds difficulties to the experiment because it requires a higher plasma temperature. The plasma model used in the derivation predicted a plasma temperature of 20 eV was required to have the 10+ charge state dominate and a 100-eV temperature was required to have a 23+ charge state dominate. It is important to note that both of the electronic transitions are $M2$ transitions, unlike the nuclear transition, which is an $E3$. The difference in multipolarity between the electron and the nuclear transition decreases the theorized NEET rate. The results for the NEET rate found in Ref. [18] are intriguing. In the case of a 20-eV plasma, the predicted NEET rate was theorized to be 10^{-9} s$^{-1} < \lambda_{\mathrm{NEET}} < 10^{-4}$ s^{-1}. For a 100-eV plasma, the theorized rate increases to 10^{-6} s$^{-1} < \lambda_{\mathrm{NEET}} < 1$ s^{-1}. There are two important features to point out for these NEET rates. First, the NEET rate is significantly larger for the hotter plasma. Second, the predicted NEET rate spans 10 orders of magnitude. The different results for the NEET rate in previous experiments may be attributable to the different plasma temperatures produced. The enormous range demonstrates the limitations of the theory. However, the results do point to the need for a plasma that is hot enough to produce uranium ions with a charge state of 23+.

The second paper to focus on NEET of ^{235}U used a different plasma assumption. In Morel *et al.* [19], the plasma was modeled in local thermodynamic equilibrium (LTE). The results of the model were very similar to the results found in Ref. [18]. Both the $6p_{1/2} \rightarrow 5d_{5/2}$ transition and the $6d_{5/2} \rightarrow 6p_{1/2}$ transition produce the highest NEET rates. The predicted uranium charge states that yield the highest probability for those transitions are 11+ and 21+, respectively. The difference in plasma models may explain the difference in predicted charge states. A plot of the NEET rate dependence on both the temperature and density was produced. The plot contained two islands with larger NEET rates than their surroundings. Once again, the $6d_{5/2} \rightarrow 6p_{1/2}$ produces the highest NEET rate. The NEET rates found in Ref. [19] are more constrained than the rates found in Ref. [18]. The NEET rates span three orders of magnitude, with the largest rate being $\lambda_{\mathrm{NEET}} = 2 \times 10^{-4}$ s^{-1}. The large NEET rate occurs at plasma temperatures of approximately 100 eV and densities around one-tenth of solid density. Both theory papers are consistent

with each other and suggest that the NEET rate of ^{235}U is likely to be small.

For this experiment and previous experiments, NEET is not the only reaction that can generate the uranium isomer. Three other reactions that can produce the isomer are photoexcitation, inelastic electron scattering, and nuclear excitation by electron capture (NEEC). NEEC is similar to NEET, except that it involves a free electron being captured into a bound state and can be considered the inverse of internal conversion [26,27]. Because the natural linewidth of the isomeric state is extremely narrow, approximately 10^{-19} eV, it is unlikely the isomeric state would be directly populated. It is also unlikely that inelastic scattering would create the isomeric state directly. The competing reaction rates found in Harston and Chemin for a 100-eV plasma were less than 10^{-17} s^{-1} for direct photoexcitation of the isomeric state, of order 10^{-16} s^{-1} for inelastic electron scattering, and 10^{-11} s^{-1} for NEEC [18]. All of the competing reaction rates for direct production of the isomeric state are smaller than the theorized NEET excitation rate of 10^{-9}–1 s^{-1} found in Harston and Chemin. The competing reaction rates found in Morel *et al.* for a 100-eV plasma were approximately 6×10^{-25} s^{-1} for direct photoexcitation of the isomeric state and less than 10^{-6} s^{-1} for NEEC [19]. A calculation for the direct production of the isomeric state from inelastic electron scattering was not provided. All of the competing reaction rates for direct production of the isomeric state are smaller than the theorized NEET excitation rate of 10^{-6}–10^{-4} s^{-1} found in Morel *et al.* The most probable competing reaction that could create the isomeric state is NEEC [18,19]. However, the NEEC rate is theorized to be smaller than the NEET rate by both theory papers.

It is important to note that higher excited states in ^{235}U have significantly wider linewidths and these states can decay to the isomeric state. For these states to be populated, both electrons and photons with higher energies are required. In the case of a laser-produced plasma, the production of hot electrons is possible. Hot electrons are high-energy electrons produced by laser-plasma interactions. They can be produced by lasers with power densities greater than 10^{12} W/cm^2 and have energies measured in keV. For a Nd:YAG laser operating at 1064 nm and a power density between 10^{13} and 10^{14} W/cm^2, hot electrons would have energies of a few keV. These energies are smaller than the second excited state of ^{235}U at 13 keV, however, the high-energy tail for the hot electron distribution could possibly excite the 13-keV state, which subsequently would decay to the isomeric state producing a false NEET signal. The problem of hot electrons produced in a laser plasma was discussed in Morel *et al.* and was found to have a negligible effect on the production of the isomeric state [19].

Plasma simulations were performed to understand the plasma generated by the Nd:YAG laser. The hydrodynamic simulations were run in two dimensions with cylindrical symmetry. The laser's wavelength, pulse energy, and pulse shape matched the measured values for the experiment. The goal of the plasma simulations was to predict the number of isomers generated by each laser pulse. The number of uranium isomers produced per laser pulse was calculated using the equation

$$N_I = \frac{\rho N_A \lambda_{\mathrm{NEET}} V \Delta t}{A}, \tag{3}$$

where ρ is the density of the plasma, N_A is the Avogadro constant, λ_{NEET} is the NEET rate, V is the volume of the plasma, Δt is the length of time the plasma is in the correct ionization state, and A is the atomic mass. It was assumed that only uranium ions with a charge state of 10+ and a charge state of 23+ were able to undergo NEET. Three cases based off of the theorized NEET rates for uranium in charge states of 10+ and 23+ were generated to predict the number of isomers produced within the plasma. The first case used a conservative estimate for the NEET rate. The second case had the NEET rate set to a value that would produce the highest number of isomers. The third case used NEET rates near the upper limit found in Ref. [8]. Table I shows the NEET rates and the predicted number of isomers produced for each case. One can see that the expected number of isomers produced per laser shot is very small except in Case 2. Case 2 uses a rate similar to the rate claimed in Izawa and Yamanaka [5]. If the rate found in Izawa *et al.* is accurate, 30 laser shots would produce an activity of 900 Hz from ^{235m}U decay. That signal would be easily observed. Both Case 1 and Case 3 produced a small quantity of isomers. The ability to determine the existence of the isomeric decay in the data for these cases is challenging and requires very good sensitivity for the experiment.

TABLE I. Number of isomers produced per laser shot from the uranium laser-plasma simulation. These cases span the predicted NEET excitation rate found in Ref. [18].

Case No.	U^{10+} λ_{NEET} (s^{-1})	U^{23+} λ_{NEET} (s^{-1})	^{235m}U produced per laser shot
Case 1	10^{-9}	10^{-6}	0.066
Case 2	10^{-4}	1	6.46×10^4
Case 3	10^{-6}	10^{-6}	1.80

III. EXPERIMENT

A. Experimental design

The general procedure for the experiment is as follows. A Nd:YAG laser operating at the fundamental wavelength of 1064 nm was used to generate the uranium plasma. The laser light was focused within the experimental chamber onto a sample of uranium on a translation stage. The target was translated during the laser irradiation. The resulting plasma plume was captured on a catcher plate. The catcher plate was raised to the top of the chamber where the detection apparatus, consisting of an electrostatic focusing lens system and a microchannel plate detector, was located. The low-energy electrons emitted from the catcher plate were counted to look for a signal consistent with the decay of ^{235m}U.

A diagram of the experimental setup is shown in Fig. 1. The laser light reflected off of three mirrors before entering the chamber. The small amount of light transmitted through the first mirror was used to monitor the laser power.

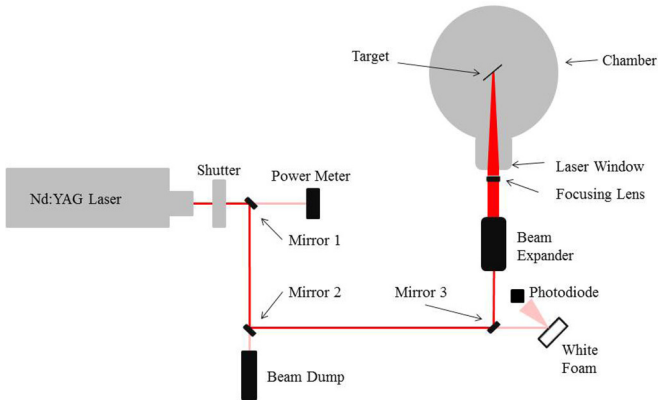

FIG. 1. Optical setup for the main experiment. The power meter and photodiode were used to measure the characteristics of the laser beam during the experiment.

The light transmitted through the third mirror was reflected off of a piece of foam to scatter the light into an InGaAs photodetector. This allowed for the counting of each laser pulse entering the chamber in addition to measuring the pulse shape. Before entering the chamber, the laser light was expanded through a Galilean telescope. The light was then focused into the chamber using a plano-convex focusing lens with a focal length of 350 mm.

The Nd:YAG laser output 790-mJ pulses with a full width at half maximum of 9 ns. While the laser could operate with a 10-Hz repetition rate, the experiment was run using single-shot mode to control the number and frequency of pulses hitting the target. The spot size on target was measured to be 50 by 100 μm. The elliptical shape was attributable to the laser light hitting the uranium target at 45°. Within the chamber, the target was held by a target holder attached to a linear translation stage. The target was enclosed by a containment box with a hole to allow the laser light to hit the target and a slit on the top to allow the catcher plate to move in and out of position. The purpose of the containment box was to minimize contamination of the chamber and to minimize the amount of light and electrons hitting the detector during irradiation. The resulting plasma plume from the laser irradiation was captured on a catcher plate held at +4 V to suppress exoelectron emission. Exoelectrons are low-energy electrons emitted from a surface that has been agitated. The agitation could be from particle impact, vacuum changes, light, or heating of the surface [28]. Exoelectron emission has a half-life that is dependent on many factors such as oxide layers, pressure, temperature, and the surface material. Exoelectron emission is a possible explanation for the discrepant results for NEET of ^{235}U. Initially, copper was used as a catcher plate. Tests using gold foils showed a reduction in the electron signal emanating from the catcher plate following laser irradiation of a target. Subsequently, the catcher plates used during the experiment were composed of copper with a thin layer of evaporated gold.

The catcher plate was attached to a linear translation arm that allowed for the catcher plate to move from the bottom of the chamber, where the laser irradiation occurred, to the top of the chamber. The chamber was divided into a top and bottom section by a painted aluminum baffle. The bottom of the baffle was painted with a black vacuum paint to absorb light from the laser irradiation. A slit in the middle of the baffle allowed the catcher plate to move from the top to the bottom of the chamber. A plug was attached to the top of the catcher plate that covered the slit in the baffle when the catcher plate was located at the bottom of the chamber. The plug helped to prevent light from triggering the detector located at the top of the chamber.

The top of the chamber consisted of a turbomolecular pump, residual gas analyzer, cold cathode vacuum gauge, electrostatic focusing lens, and a microchannel plate (MCP) detector. The electrostatic focusing lens was designed and built to accelerate and focus the low-energy electrons from the decay of ^{235m}U onto the MCP detector. The lens consisted of five aluminum rings and a metal grid. The program SIMION was used to optimize the voltage found on each of the lens components to optimize the detection efficiency for the low-energy electrons emitted from the catcher plate while preventing background electrons from hitting the detector [29]. The microchannel plate detector was a Photonis APD 2 MA 18/12/10/8 D 60:1 Grid. It was a chevron design with an active diameter of 18 mm. The front of the MCP detector was held at +1471 V. This was done to maximize the detection efficiency of the MCP detector for seeing electrons.

The signal from the MCP detector was sent to a passive splitter. One output of the splitter was used to generate a gate. Owing to the ringing of the MCP signal, a veto circuit was designed. A 15-μs dead time was established to prevent multiple signals from the same electron cascade from being digitized by the analog-to-digital converter (ADC). The gate generated by the initial signal was sent to an Ortec ASPEC-927 multichannel analyzer (MCA). The second output of the passive splitter was sent to an amplifier before being sent to the MCA. The data was collected using an automated job file. The ADC recorded 1-min spectra over the course of 10–16 h.

B. Uranium samples

Several uranium samples were used during this experiment. Owing to the known problem of exoelectrons [8], two types of uranium samples were used. The two types were the null uranium samples and the enriched uranium samples. The null samples were either composed of natural uranium or depleted uranium. Owing to their low concentration of ^{235}U, no signal or a small signal of the isomeric decay was expected to be observed. If the decay of ^{235m}U was observed, the amount of ^{235m}U generated using the enriched samples should be proportional to the ^{235}U concentration given the same experimental conditions. If the signal was not proportional, the observed decay would either be attributable to electron emission unrelated to ^{235m}U decay, or the experimental conditions were not similar. Table II lists the uranium samples used during the experiment.

The samples of enriched uranium used during the experiment were enriched to either 93% or 99.4% ^{235}U. Because the expected signal was small, minimizing background was a priority. The concentrations of both ^{234}U and ^{236}U in 93% uranium made the expected α background very large. While it was unlikely that the α decays would directly hit the MCP

TABLE II. Natural, depleted, and enriched uranium samples used during the experiment. The mass for each sample is given along with the nominal mass fraction isotopics for the two main isotopes within the sample.

Sample name	Mass (g)	^{235}U(%)	^{238}U(%)
DU metal	0.7	0.2	99.8
NU ceramic 1	0.507	0.7	99.3
NU ceramic 2	0.297	0.7	99.3
Binary metal	1.3	0.2	99.8
DU carbide	0.410	0.2	99.8
HEU ceramic	0.275	99.44	0.0497
HEU metal	0.299	93	5.5
HEU carbide	0.290	99.44	0.0497

detector, the release of δ electrons from the α decay was a significant source of background counts. The specific activity of the 99.4% uranium was 13 times smaller than the specific activity of the 93% uranium. Because the 99.4% uranium had a significantly smaller specific activity and it had a higher proportion of ^{235}U, it was the preferred enriched uranium sample. However, the 99.4% enriched uranium obtained was a powder. Because the enriched uranium was powder, the material had to be turned into a solid form. This resulted in the creation of two targets. One target was an enriched uranium oxide puck and the other target was an enriched uranium carbide pellet. In addition to the above enriched targets, a metal sample of 93% enriched uranium was also obtained.

Multiple null targets were created to match the chemical forms of the enriched uranium targets. Two types of uranium metal targets for the null tests were obtained. The first was a sample of depleted uranium metal. The second was a depleted uranium binary metal puck that consisted of 94% uranium and 6% niobium. Two uranium oxide ceramic pucks were created using the same pressing and sintering method used to create the enriched uranium oxide pucks. The brittleness and low density of the uranium oxide pucks made them poor targets for laser irradiation. Only limited tests were performed using the uranium oxide pucks owing to their inability survive multiple laser pulses.

To prepare dense, metallic samples, mixed oxides of depleted and enriched uranium were combined to form two separate uranium-carbide samples. The uranium oxides powders were reduced to UO_2 by heating at 650°C for 24 h in a tube furnace with flowing ultrahigh-purity H_2. The resulting oxide powders were black in color, and x-ray diffraction measurements indicated UO_2. For both enrichments, the UO_2 was then weighed and combined with graphite such that the following reaction could proceed once heated: $UO_2 + 3C \rightarrow 2CO + UC$. Excess graphite was included to ensure that the reaction had sufficient carbon to occur. The mixed powders were ground with a mortar and pestle and loaded into a die, which was then loaded with 8000 lb of force, yielding a lightly packed pellet of UO_2/graphite powder. The pellets were then transferred to an arc furnace, where they were heated until the reaction above proceeded, which resulted in a metallic boule of material. The boule was melted and flipped three times and then allowed to cool. Any excess graphite from the mixing procedure above could be incorporated into the melt to form some UC_2. X-ray diffraction analysis of the samples showed that the depleted UO_2 was converted to a 50-50 mixture of UC and UC_2, whereas the enriched UO_2 was converted to UC with no more than 10% UC_2 impurities. X-ray diffraction data along with pictures of the process used to create the uranium carbide target are shown in Fig. 2.

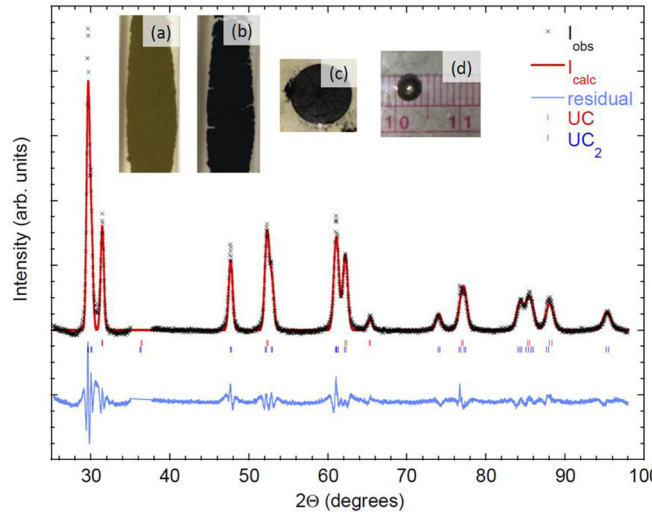

FIG. 2. X-ray diffraction data (black symbols) for a uranium carbide sample synthesized from depleted uranium oxide. The solid red line is the refinement, the solid blue line along the bottom is the residual (observed-calculated), and the red and blue tick marks below the pattern represent the locations of the Bragg peaks for UC and UC_2, respectively. The refinement implies a 50:50 mixture of UC:UC_2. The inset shows images from the synthesis process: (a) as-received, yellow-brown mixed oxide; (b) black UO_2 powder after heating in ultra-high-purity H_2; (c) pressed pellet of UO_2+graphite; and (d) the metallic boule of uranium carbide after melting.

C. Uranium ablation experiments

Two experiments were performed to determine the amount of ablated material captured on the catcher plate per laser shot. The first experiment was performed in a small test chamber using depleted uranium metal. The experiment determined both the distribution and the total amount of ablated material on the catcher plate. The catcher plate for the first experiment consisted of a 2.1″ square copper catcher plate cut into nine equal-sized squares. The squares were then recombined to make the original square copper plate. The purpose of cutting the plate into smaller squares was to allow for each individual square to be measured, allowing for the plume distribution on the catcher plate to be determined. A total of 1250 laser shots hit the target. An Ortec Soloist Alpha Spectrometer was used to measure the total amount of uranium found on each individual copper square. The detector was calibrated using a ^{226}Ra α source. The total amount of mass ablated was 1103 ± 16 μg, which equates to 883 ± 18 ng per laser shot captured on the catcher plate. The plume was determined to be forward peaked with a majority of the ablated uranium being found on the central copper square.

The second experiment determined the amount of uranium deposited on the catcher plate per laser shot within the experimental chamber using the uranium binary metal target. Unlike the ablation experiment performed in the test chamber, this experiment was run with the exact same setup used for the main experiment looking for NEET of ^{235}U. A total of 939 shots hit the uranium target. The catcher plate was removed from the chamber and α spectroscopy was performed to determine the total amount of uranium ablated. An Ortec B-Series Totally Depleted Silicon Surface Barrier Detector calibrated using a ^{226}Ra α source was used to determine the total amount of uranium found on the catcher plate. The total amount of uranium on the catcher plate was determined to be 647 ± 23 μg. Because the uranium binary target contained 6% niobium, the total mass ablated per laser shot, correcting for the niobium content, was 733 ± 26 ng. The difference in mass ablated between the first ablation experiment and the second can be attributed to the difference in solid angle coverage owing to the catcher plate being farther away from the target in the experimental chamber than it was in the test chamber.

IV. RESULTS

A. Efficiency

One of the most difficult aspects of the experiment was measuring the detection efficiency for observing low-energy electrons emitted from the catcher plate. To measure the efficiency for observing electrons from the decay of ^{235m}U, a 5.4-μCi ^{239}Pu source was used. ^{239}Pu decays to ^{235m}U nearly 100% of the time. The ^{235m}U nuclei from the α decay of ^{239}Pu have an energy greater than 80 keV. When collected at vacuum, the ^{235m}U recoils embed into the catcher plate. Owing to the short path length for eV electrons, the low-energy electrons are significantly attenuated. The uranium ions generated during laser ablation would have energies of order 100 eV. The ions would not embed as deeply into the surface of the catcher plate owing to their lower energy. To correct for this, the collection of ^{235m}U recoils was performed with the chamber containing 2 Torr of argon gas. The recoils were stopped in the gas and a small electric field was applied to the catcher plate to collect the ^{235}U recoils on the surface. The recoils were collected at the bottom of the chamber. Knowing both the source strength and the solid angle allowed for the total number of recoils on the catcher plate to be determined. The catcher plate was raised to the top of the chamber and a decay spectrum was obtained for the decay of ^{235m}U. Figure 3 shows the decay spectrum for ^{235m}U produced by ^{239}Pu decay. The detection efficiency for observing the decay of ^{235m}U on the catcher plate was determined to be 0.051 ± 0.003.

The above determination for the detection efficiency assumed that the ^{235m}U was on the surface of the catcher plate. During the experiment, the laser-ablated uranium would form a layer on the catcher plate surface that would attenuate the signal from ^{235m}U decay. Owing to a thick layer of uranium attenuating the signal, the number of laser shots per experimental run was limited to under 40 shots. To account for the attenuation of the signal, a correction factor (CF) for the efficiency was determined. The correction factor is given by

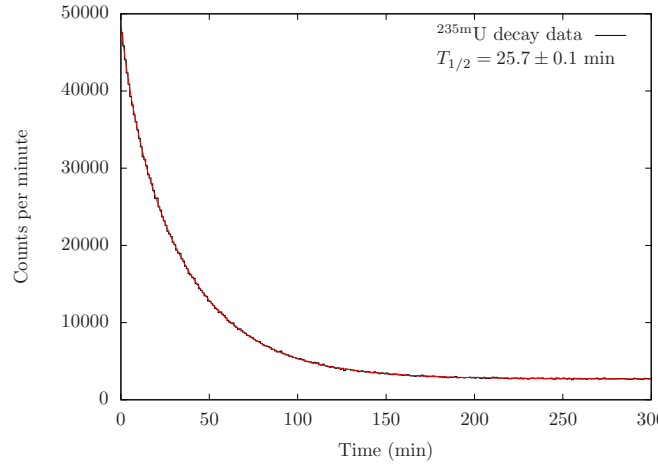

FIG. 3. Decay of ^{235m}U produced by the decay of ^{239}Pu. The uranium recoils were slowed in argon gas and were collected for 2 h.

the equation

$$CF = 1/T \int_0^T \int_0^{\pi/2} \exp\left[\frac{-t}{\lambda(t,\theta)\cos(\theta)}\right] \sin(\theta) d\theta dt, \quad (4)$$

where T is the total thickness of the layer, θ is the angle of emission for the electron, and $\lambda(t,\theta)$ is the effective attenuation length (EAL) for the electrons through the material. The values for the practical EAL for 50-eV electrons through uranium were obtained from the National Institute of Standards and Technology (NIST) Standard Reference Database 82 [30]. The minimum energy for electrons within the NIST database was 50 eV. The ablation experiment that determined the distribution of the uranium on the catcher plate was used to determine the thickness of the uranium layer on the catcher plate. A correction factor for each of the nine segments was determined and then averaged to obtain a total correction factor for the efficiency of 0.481 when 30 laser shots were performed. When applied to the efficiency found using the ^{239}Pu source, the detection efficiency for seeing the decay of ^{235m}U was determined to be 0.025 ± 0.003.

B. Uranium metal experiments

Irradiation of the depleted uranium metal target produced multiple decays in the spectrum. The spectrum was fit with two exponential functions and a background. The spectrum consisted of a fast decay with a half-life of 3.49 ± 0.27 min along with a slow decay with a half-life of 20.6 ± 0.7 min. There was no evidence of ^{235m}U decay. The depleted uranium binary target produced similar results. A fast decay with a half-life of 4.6 ± 0.7 min and a slow decay with a half-life of 40.9 ± 10.7 min were observed. There was no evidence of a 26-min decay one would expect if ^{235m}U was generated. Both targets mentioned above contained depleted uranium and were null targets to compare to the enriched metal target. The HEU metal target was irradiated under similar conditions to the null targets. Once again, two decays in the spectrum were observed. The spectrum consisted of a fast decay with a half-life of 1.73 ± 0.55 min and a slow decay with a half-life of

16.4 ± 3.0 min. No evidence of ^{235m}U decaying was observed. The presence of fast and slow decays using both the null and the enriched targets suggests the observed decays were unrelated to the enrichment of the targets and were likely attributable to exoelectrons.

C. Uranium ceramic experiments

The uranium ceramic experiments consisted of multiple runs using two different uranium ceramic null targets and one enriched uranium ceramic target. Irradiation of the ceramic targets was problematic owing to their poor thermal properties and brittleness. Only a few runs on each target was possible. Spectra generated after irradiation of the natural uranium ceramic targets consisted of multiple decays. Unlike the metal targets, the spectra were best fit with three exponential decays and a background. The spectrum from the first natural uranium ceramic target consisted of a fast decay with a half-life of 1.13 ± 0.29 min, a slow decay with a half-life of 10.5 ± 1.1 min, and a very slow decay with a half-life of 91.8 ± 5.9 min. The spectrum from the second natural uranium ceramic target consisted of a fast decay with a half-life of 2.54 ± 0.34 min, a slow decay with a half-life of 12.6 ± 1.9 min, and a very slow decay with a half-life of 70.1 ± 6.5 min. Both targets did not have a half-life consistent with ^{235m}U decay. The enriched uranium ceramic target was irradiated under similar conditions to the natural uranium ceramic targets. No evidence of ^{235m}U decay was observed in the enriched uranium ceramic data. A spectrum from one of the enriched uranium ceramic runs consisted of a fast decay with a half-life of 3.49 ± 0.44 min, a slow decay with a half-life of 19.66 ± 3.0 min, and a very slow decay with a half-life of 130 ± 33 min. The presence of multiple decaying systems in both the natural uranium and enriched uranium ceramic data once again points to exoelectron emission being the cause of the signal.

D. Uranium carbide experiments

The uranium carbide targets provided the best data. The carbide targets consisted of the best aspects of the metal targets and the ceramic targets, without their down sides. The carbide targets were near metal density and were not brittle. In addition, the enriched carbide target was composed of 99.4% ^{235}U, thus allowing for a higher sensitivity measurement compared to the 93% ^{235}U metal target. The carbide experiments consisted of two runs with the depleted uranium carbide target and two runs with the enriched uranium carbide target. A total of 30 laser shots hit the target during each run. Owing to a problem with the translation arm, the MCP detector was not fully operational until 14 min after the start of the laser shots. An example decay spectrum from the depleted uranium carbide experiment is shown in Fig. 4. The decay data were best fit using three exponential functions plus a background. The decay spectrum consisted of a fast decay with a half-life of 6.15 ± 0.52 min, a slow decay with a half-life of 31.8 ± 1.8 min, and a very slow decay with a half-life of 151 ± 9 min. There was no evidence of the 26-min decay associated with ^{235m}U decay. The data contained nonstatistical counts and occasional spikes. These point to a systematic problem during the experiment.

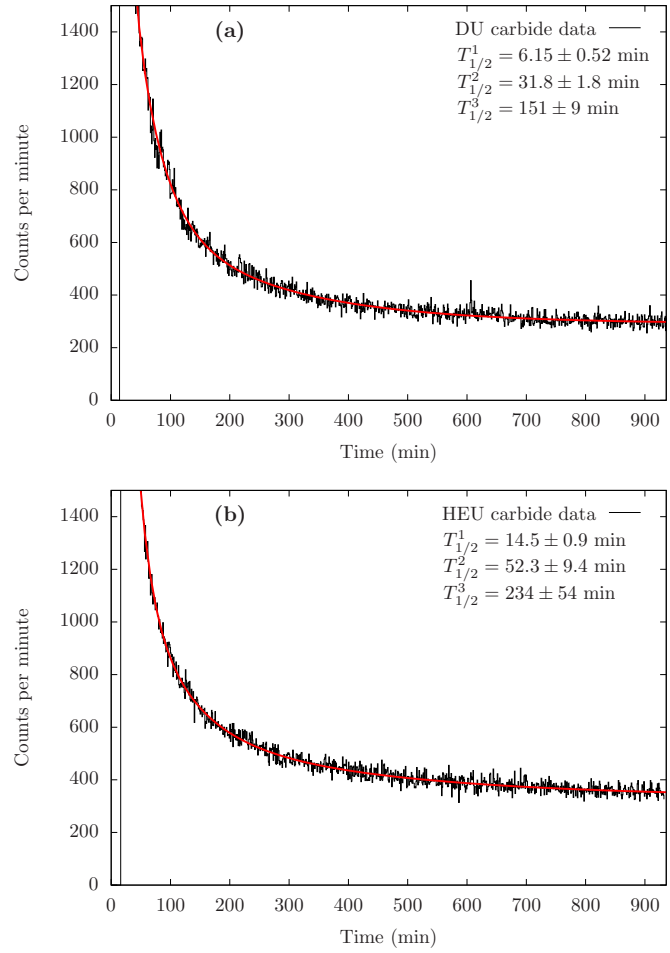

FIG. 4. Decay spectra from the carbide experiments. Spectrum (a) is a decay spectrum from one of the DU carbide runs. Spectrum (b) is a decay spectrum from one of the HEU carbide runs. Time zero is the start of the laser shots. The detector was fully operational 14 min after the start of the laser shots.

The enriched uranium carbide target was irradiated under similar conditions to the depleted uranium carbide target. Two runs were performed each with 30 shots on target. An example spectrum from one of the runs is shown in Fig. 4. The spectrum was best fit using three exponential functions plus a background. The decay spectrum did not contain a very fast decay. The half-lives from the fit to the data were 14.5 ± 0.9, 52.3 ± 9.4, and 234 ± 54 min. No evidence of ^{235m}U was observed. The half-lives measured were different than the half-lives measured using the depleted uranium carbide target. This difference can be attributed to multiple factors. Although both the depleted uranium and enriched uranium carbide targets were produced using the same procedure, the oxygen and carbon content in the targets were different. Additionally, nonstatistical counts in the spectra were observed.

To determine if the ^{235m}U signal was hidden within the data, both depleted uranium carbide data sets were summed. In addition, both enriched uranium carbide data sets were summed. The summed depleted uranium carbide data set was scaled to the summed enriched uranium carbide data set

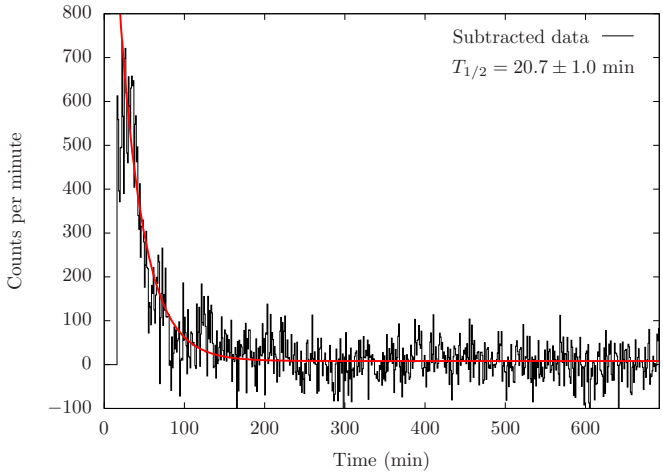

FIG. 5. Enriched uranium carbide decay spectrum after subtraction of the depleted uranium decay spectrum.

and subsequently subtracted from summed enriched uranium carbide data set. If there were no nonstatistical effects, the resulting spectra would be flat, assuming they were properly scaled. The resulting spectrum from this process is shown in Fig. 5. Although all of the spectra that were added and subtracted to make the spectrum were collected using the same experimental conditions, there is still a decay present in the resulting spectrum. This suggests there is an unknown systematic effect in the experiment. The subtraction of the depleted data from the enriched data removed all but one decay. The half-life of the remaining decay was 20.7 ± 1.0 min. There was no evidence of a 26-min decay within the data. If the isomer was created, its signal was hidden beneath the remaining decay.

E. Data analysis

To determine the upper limit for the NEET excitation rate of ^{235}U, the minimum number of isomers that needed to be created for the decay to be visible within the data was determined. This was accomplished using a method found in Ref. [31]. To account for the unknown systematic effect occurring during the experiment, the error bars were expanded by the square root of the reduced χ^2. The data were fit with an equation consisting of two exponential functions plus a background. One of the exponential functions had a fixed half-life of 26 min. Initially, it was assumed there were no isomers present and the total χ^2 was determined for the fit. By perturbing the initial amount of uranium isomers present in the fit and then fitting the data, the total χ^2 would increase. When the total χ^2 increased by 1.00, that determined the minimum number of isomers that one could see in the spectrum with a confidence level of 68.3%. Using this method, the minimum number of isomers able to be detected was found to be 3540. It should be noted that the minimum number of isomers determined using this method assumes a detection efficiency of 100%. This has to be corrected for when calculating the upper limit for NEET of ^{235}U.

TABLE III. Parameters used to calculate the NEET upper limit along with their uncertainties.

Variable name	Value	Uncertainty (%)
N_{235}	1.06×10^{17} atoms	11
τ	9×10^{-9} s	1
ϵ	0.025	11

The upper limit for the NEET excitation rate of ^{235}U averaged over the laser pulse is given by

$$\lambda_{\mathrm{NEET}} = \frac{N_{235\mathrm{m}}}{N_{235}\tau\epsilon}, \tag{5}$$

where $N_{235\mathrm{m}}$ is the minimum number of isomers necessary to make the decay visible in the data, N_{235} is the number of ^{235}U atoms on the catcher plate, τ is the width of the laser pulse, and ϵ is the detection efficiency. Table III contains the values for the variables used in the above equation along with their uncertainties. To account for the uncertainties in the values, the 1σ lower limit for the denominator of Eq. (5) was used. This approach produces a conservative estimate of the limit. The upper limit for the NEET rate of ^{235}U with a confidence level of 68.3% was determined to be $\lambda_{\mathrm{NEET}} < 1.8 \times 10^{-4}$ s^{-1}.

V. DISCUSSION

The upper limit for the NEET rate of ^{235}U determined from this experiment of $\lambda_{\mathrm{NEET}} < 1.8 \times 10^{-4}$ s^{-1} can be compared to previous measurements looking for NEET of ^{235}U. The NEET rate found in Izawa and Yamanaka [5] was approximately 0.1 s^{-1}. Correcting for the plasma assumptions would yield a rate of approximately 2 s^{-1} [18]. No subsequent experiments looking for NEET of ^{235}U observed that large of a rate. The experiment discussed in this article used natural, depleted, and enriched uranium and did not observe any signal consistent with $^{235\mathrm{m}}$U decay. It is unlikely that NEET of ^{235}U was observed in Izawa *et al.* The explanation for the fast decay seen in their spectra being attributable to α emission is improbable owing to the low activity of natural uranium and the time it takes for free floating uranium to plate out on a surface. The fast decay may have been attributable to either fluorescence of their channeltron detector or exoelectron emission from their catcher plate. Although a half-life consistent with $^{235\mathrm{m}}$U was observed, exoelectron emission cannot be excluded as the source of their slow decaying signal. In addition, numerous assumptions were made for their plasma conditions that make assigning an excitation rate for their experiment very difficult. All of these factors suggest the measured signal reported by Izawa *et al.* was, in fact, not from $^{235\mathrm{m}}$U decay.

The experiments described in Arutyunyan *et al.* [7] reported different results. The first experiment using a 5-J CO_2 laser did not observe NEET of ^{235}U. A limit for the cross section was reported that corresponds to an excitation rate limit of $\lambda_{\mathrm{NEET}} < 10^{-5}$ s^{-1} [18]. This limit is consistent with the limit set in this article. Unlike the experiment described in Ref. [5], the sample was 6% enriched UO_2. The increase in the amount of ^{235}U should have provided a clear NEET

signal. The lack of signal furthers the point that NEET of ^{235}U was not observed in Ref. [5]. Very little is known about the experimental setup and the plasma conditions for this experiment. This makes comparisons to the other uranium NEET experiments difficult. The second experiment described in their article involved the use of a high-energy electron gun to generate a uranium plasma. Intense pulses of 500-keV electrons bombarded a variety of uranium targets. The targets were either depleted or enriched in ^{235}U. Between 5 and 20 experiments were run with each target. Only the targets with enrichment of 93.4% ^{235}U and 99.99% ^{235}U showed evidence of a decay. The NEET rate was determined to be approximately 3×10^{-5} s^{-1} [18]. While this rate is consistent with the limit set in this article, it is significantly less than the rate found in Ref. [5]. The presence of high-energy electrons during their experiment allowed for reactions to occur that populate higher-lying states. Photoexcitation, inelastic electron scattering, and NEEC all could have generated the isomer. Calculations found in Ref. [18] suggest that the most likely reaction to produce the isomer was inelastic electron scattering with an excitation rate of approximately 10^{-7} s^{-1}. The excitation rate is significantly larger than the rate presented in Sec. II owing to higher-lying nuclear states being populated and decaying to the isomeric state. Inelastic electron scattering does not fully account for the rate observed by Arutyunyan *et al.* In addition, no attempt was made to measure the energies of the electrons emitted. The possibility that exoelectrons generated the signal cannot be dismissed. Interestingly, many of the runs that were claimed to contain the isomeric decay had either half-lives inconsistent with the half-life of ^{235m}U, or very large uncertainties in the value of the half-life. It was claimed that the variations observed during the experiments were directly related to the beam focus. While this could account for the differences in the number of decaying systems measured, it does not explain the large variations in half-lives. The electron beam experiment performed by Arutyunyan *et al.* provides an inconclusive result. While NEET of ^{235}U may have occurred, the competing reactions and the large variations in half-lives measured suggest that other mechanisms were responsible for their signal. The most likely explanation for the signal is a combination of isomers produced by inelastic electron scattering and the presence of exoelectron emission. The large variation in the half-lives measured in Arutyunyan *et al.* is very similar to the variations in the measured half-lives found in this experiment for the various targets. This experiment attributed the variation to exoelectron emission and that is also a likely candidate for the signal observed in Arutyunyan *et al.*

The results of this article are consistent with the upper limit of $\lambda_{\mathrm{NEET}} < 6 \times 10^{-6}\,\mathrm{s}^{-1}$ found in Claverie *et al.* [8]. This experiment and the one described in Claverie *et al.* were very similar. Both used Nd:YAG lasers, gold catcher plates, and enriched uranium targets. The presence of plasma diagnostics during their experiment allowed for additional information to be collected. The estimated power density on target from Ref. [8] was 10^{13} W/cm^2. This is an order of magnitude larger than the estimated power density for this experiment. This would suggest the experiment performed by Claverie *et al.* and the one described in this article would have different plasma conditions. The plasma simulation described in this article had a dense plasma region with a charge state near 23+. This is with the order-of-magnitude-lower power density on target. This would suggest that the charge state of uranium during the experiment described in Claverie *et al.* was significantly higher than what was expected. The problem of exoelectrons was thoroughly discussed in Ref. [8]. Before attempts were made to mitigate exoelectron emission, both a fast decay with a half-life of 2.9 min and a slow decay with a half-life of 25.5 min were observed in their data. The slow decay had a half-life similar to the half-life of ^{235m}U, which may explain the discrepant results from previous experiments. By switching the catcher plate to gold and applying +2 V to the plate, it was claimed that the decay signals were eliminated. While the exoelectron signal was reduced, decays were still visible in the plot provided. The calculation used to determine the NEET limit was not fully described in Claverie *et al.* What is known is that ten independent measurements were added together. It was assumed that the experimental runs were exactly the same. What is clear from this article is that different runs using the exact same conditions did not produce the exact same results. An unknown systematic issue could have been present that changes after each run. To determine the upper limit, a perfect decay distribution was added to the data to determine the minimum number of isomers visible in the data. There was no discussion about how they determined the minimum number of isomers they could extract from the data. It was assumed that the summed data were flat. This assumption may not be true considering the application of +2 V on their gold catcher plate did not completely remove the exoelectron signal. In addition, there appears to be a slight positive slope to their summed data. Both effects would limit the ability to ascertain the minimum number of isomers that would be visible in the data. While it is clear there was no observation of the isomer in their data, it is unlikely their upper limit is as stringent as claimed.

While it is likely that past observations of NEET in ^{235}U were either attributable to mischaracterization of the signal or competing reactions, there exists the possibility that all measurements were, in fact, correct. The narrow resonance that allows for NEET of ^{235}U to occur is heavily dependent on the plasma conditions generated. Only in Ref. [8] was an attempt made to measure the plasma conditions present during the experiment. If all of the experiments generated different plasma conditions, it is possible all of the experiments would have encountered a different NEET rate. Without measurements of the plasma conditions generated during the experiments, this conclusion cannot be excluded.

VI. CONCLUSION

An upper limit for the NEET excitation rate of ^{235}U was determined to be $\lambda_{\mathrm{NEET}} < 1.8 \times 10^{-4}$ s^{-1}. This limit is consistent with all past experiments except for Izawa *et al.* The discrepancy between this measurement and Izawa *et al.* is likely attributable to a mischaracterization of their signal. Uranium targets with different amounts of ^{235}U enrichment were used and no evidence of NEET of ^{235}U was observed. There are numerous improvements necessary for future measurements attempting to measure NEET of ^{235}U. The most important improvement would be the inclusion of multiple

plasma diagnostics to measure the ion density, temperature, and charge state of the plasma. Matching the plasma state to the experimental conditions present would remove the possibility that some of the discrepant results observed over the past 40 yr were attributable to differing plasma conditions. The presence of exoelectrons suggests the need for an electron spectrometer to suppress electron events not associated with ^{235m}U decay. Finally, increasing the efficiency of the system to detect low-energy electrons would increase the sensitivity of the experiment. These improvements would not only increase the sensitivity of future measurements, but would also provide information necessary to improve NEET theory.

ACKNOWLEDGMENTS

This work was performed under the auspices of the US Department of Energy by Lawrence Livermore National Laboratory under Contract No. DE-AC52-07NA27344. This research was additionally performed under appointment to the Nuclear Nonproliferation International Safeguards Graduate Fellowship Program sponsored by the National Nuclear Security Administration's Next Generation Safeguards Initiative (NGSI). This work was further supported by the US Department of Homeland Security, UC Berkeley, and the Nuclear Science and Security Consortium under DOE Contract No. DE-NA-0000979.

[1] M. Morita, Nuclear excitation by electron transition and its application to Uranium 235 separation, Prog. Theor. Phys. **49**, 1574 (1973).

[2] S. Kishimoto, Y. Yoda, M. Seto, Y. Kobayashi, S. Kitao, R. Haruki, T. Kawauchi, K. Fukutani, and T. Okano, Observation of Nuclear Excitation by Electron Transition in ^{197}Au with Synchrotron X Rays and an Avalanche Photodiode, Phys. Rev. Lett. **85**, 1831 (2000).

[3] S. Kishimoto, Y. Yoda, Y. Kobayashi, S. Kitao, R. Haruki, R. Masuda, and M. Seto, Nuclear excitation by electron transition on ^{197}Au by photoionization around the K-absorption edge, Phys. Rev. C **74**, 031301 (2006).

[4] S. Kishimoto, Y. Yoda, Y. Kobayashi, S. Kitao, R. Haruki, and M. Seto, Evidence for nuclear excitation by electron transition on ^{193}Ir and its probability, Nucl. Phys. A **748**, 3 (2005).

[5] Y. Izawa and C. Yamanaka, Production of ^{235}U^{m} by nuclear excitation by electron transition in a laser produced uranium plasma, Phys. Lett. B **88**, 59 (1979).

[6] Y. Izawa, H. Otani, and C. Yamanaka, Nuclear excitation of uranium 235 by electron transition in laser produced uranium plasma, in *Laser Interaction and Related Plasma Phenomena*, edited by H. J. Schwarz, H. Hora, M. J. Lubin, and B. Yaakobi (Plenum, New York, 1981), Vol. 5, Chap. 2, pp. 289–299.

[7] R. V. Arutyunyan, L. A. Bol'shov, V. D. Vikharev, S. A. Dorshakov, V. A. Kornilo, A. A. Krivolapov, V. P. Smirnov, and E. V. Tkalya, Cross section for excitation of the isomer ^{235m}U in the plasma produced by an electron beam, Yad. Fiz. **53**, 36 (1991).

[8] G. Claverie, M. M. Aléonard, J. F. Chemin, F. Gobet, F. Hannachi, M. R. Harston, G. Malka, J. N. Scheurer, P. Morel, and V. Méot, Search for nuclear excitation by electronic transition in ^{235}U, Phys. Rev. C **70**, 044303 (2004).

[9] V. I. Zhudov, V. M. Kulakov, B. V. Odinov, and A. D. Panov, in *Accurate Measurements in Nuclear Spectroscopy* (Mokslas, Lithuania, 1984), pp. 109–111.

[10] H. Fujioka, K. Ura, A. Shinohara, T. Saito, and K. Otozai, Observation of nuclear excitation by electron transition (NEET) in ^{197}Au, Z. Phys. A **315**, 121 (1984).

[11] K. Otozai, R. Arakawa, and T. Saito, Nuclear excitation by electron transition in ^{189}Os, Nucl. Phys. A **297**, 97 (1978).

[12] A. Shinohara, T. Saito, M. Shoji, A. Yokoyama, H. Baba, M. Ando, and K. Taniguchi, Nuclear excitation in ^{189}Os with synchrotron radiation, Nucl. Phys. A **472**, 151 (1987).

[13] T. Saito, A. Shinohara, and K. Otozai, Nuclear excitation by electron transition (NEET) in ^{237}Np following K-shell photoionization, Phys. Lett. B **92**, 293 (1980).

[14] M. de Mevergnies and P. D. Marmol, Effect of the oxidation state on the half-life of ^{235}U^{m}, Phys. Lett. B **49**, 428 (1974).

[15] M. N. de Mévergnies, Chemical Effect on the Half-Life of U^{235m}, Phys. Rev. Lett. **23**, 422 (1969).

[16] M. N. de Mevergnies, Perturbation of the ^{235m}U Decay Rate by Implantation in Transition Metals, Phys. Rev. Lett. **29**, 1188 (1972).

[17] P. A. Chodash, Nuclear Excitation by Electronic Transition of ^{235}U, Ph.D. thesis, University of California, Berkeley, 2015.

[18] M. R. Harston and J. F. Chemin, Mechanisms of nuclear excitation in plasmas, Phys. Rev. C **59**, 2462 (1999).

[19] P. Morel, V. Méot, G. Gosselin, D. Gogny, and W. Younes, Evaluation of nuclear excitation by electronic transition in ^{235}U plasma at local thermodynamic equilibrium, Phys. Rev. A **69**, 063414 (2004).

[20] E. V. Tkalya, Mechanisms for the Excitation of Atomic Nuclei in Hot Dense Plasma, Laser Phys. **14**, 360 (2004).

[21] P. Morel, V. Méot, G. Gosselin, G. Faussurier, and C. Blancard, Calculations of nuclear excitation by electron capture (NEET) in nonlocal thermodynamic equilibrium plasmas, Phys. Rev. C **81**, 034609 (2010).

[22] E. V. Tkalya, Nuclear excitation in atomic transitions (NEET process analysis), Nucl. Phys. A **539**, 209 (1992).

[23] E. V. Tkalya, Probability of nonradiative excitation of nuclei in transitions of an electron in an atomic shell, Sov. Phys. JETP **75**, 200 (1992).

[24] E. V. Tkalya, Theory of the nuclear excitation by electron transition process near the K edge, Phys. Rev. A **75**, 022509 (2007).

[25] M. Harston, Analysis of probabilities for nuclear excitation by near-resonant electronic transitions, Nucl. Phys. A **690**, 447 (2001).

[26] V. Goldanskii and V. Namiot, On the excitation of isomeric nuclear levels by laser radiation through inverse internal electron conversion, Phys. Lett. B **62**, 393 (1976).

[27] A. Pálffy, W. Scheid, and Z. Harman, Theory of nuclear excitation by electron capture for heavy ions, Phys. Rev. A **73**, 012715 (2006).

[28] F. Brotzen, Emission of Exoelectrons from Metallic Materials, Phys. Status Solidi B **22**, 9 (1967).

[29] D. A. Dahl, SIMION for the personal computer in reflection, Int. J. Mass Spectrom. **200**, 3 (2000).

[30] C. J. Powell and A. Jablonski, *NIST Electron Effective-Attenuation-Length Database-Version 1.3* (National Institute of Standards and Technology, Gaithersburg, Md, 2011).

[31] W. H. Press, S. A. Teukolsky, W. T. Vetterlong, and B. P. Flannery, *Numerical Recipes in C++: The Art of Scientific Computing*, 2nd ed. (Cambridge University Press, Cambridge, UK, 2002).